

Impact of transcranial direct current stimulation on cognitive function, brain functional segregation, and integration in patients with mild cognitive impairment according to amyloid-beta deposition and *APOE* ϵ 4-allele

Dong Woo Kang

Seoul Saint Mary's Hospital

Sheng-Min Wang

Seoul Saint Mary's Hospital

TaeYeong Kim

NEUROPHET Inc.

Donghyeon Kim

NEUROPHET Inc.

Hae-Ran Na

Gatollik Daehakgyo Yeouido Seongmo Byeongwon: Catholic University of Korea Yeouido Saint Mary's Hospital

Nak-Young Kim

Keyo Hospital

Chang Uk Lee

Seoul Saint Mary's Hospital

Hyun Kook Lim (✉ drblues@catholic.ac.kr)

Catholic University of Korea Yeouido Saint Mary's Hospital <https://orcid.org/0000-0001-8742-3409>

Research

Keywords: amyloid beta deposition, *APOE* ϵ 4-allele, mild cognitive impairment, transcranial direct current stimulation

Posted Date: March 31st, 2021

DOI: <https://doi.org/10.21203/rs.3.rs-360532/v1>

License:  This work is licensed under a Creative Commons Attribution 4.0 International License.

[Read Full License](#)

Abstract

Background: Anodal transcranial direct current stimulation (anodal-tDCS) is known to improve cognition and normalise abnormal network configuration during resting-state functional magnetic resonance imaging (fMRI) in patients with mild cognitive impairment (MCI). We evaluated the impact of sequential anodal-tDCS on cognitive functions, functional segregation, and integration parameters in patients with MCI, according to high-risk factors for Alzheimer's disease (AD): amyloid-beta ($A\beta$) deposition and *APOE* $\epsilon 4$ -allele status.

Methods: In 32 patients with MCI ($[^{18}F]$ flutemetamol-: $n = 10$, $[^{18}F]$ flutemetamol+: $n = 22$; *APOE* $\epsilon 4$ -: $n = 13$, *APOE* $\epsilon 4$ +: $n = 19$), we delivered anodal-tDCS (2 mA/day, five times/week, for 2 weeks) over the left dorsolateral prefrontal cortex and assessed the neuropsychological test battery and resting-state fMRI measurements before and after 2 weeks' stimulation.

Results: We observed a trend for impact of an anodal-tDCS-by- $A\beta$ retention interaction on MMSE score changes. Baseline $A\beta$ accumulation tended to be negatively associated with word list recognition score changes. We found a significant effect of tDCS-by-*APOE* $\epsilon 4$ -allele interaction on changes in the functional segregation parameter of the temporal pole. Baseline $A\beta$ deposition associated negatively with change in global functional integrity of hippocampal formation. There was a significant difference in brain functional segregation and integration parameters between MCI patients with and without high-risk factors of AD.

Conclusions: Thus, anodal-tDCS could help to improve cognitive function and enhance restorative and compensatory intrinsic functional changes in MCI patients, modulated by the presence of $A\beta$ retention and the *APOE* $\epsilon 4$ -allele.

Trial registration: This study is registered with the Clinical Research Information Service of Korea Disease Control and Prevention Agency (KCT0006020). Registered on 24 March 2021—retrospectively registered.

Background

Alzheimer's disease (AD) is a leading cause of dementia and imposes a marked social and economic burden. Mild cognitive impairment (MCI), a prodromal AD stage, involves subjective and objective decline in cognitive function, but preservation of the independent daily living ability [1]. Since 10–15% of MCI patients convert to dementia annually, various attempts have been made to delay or prevent the transition to dementia at this stage [2]. Although therapeutic attempts, such as cognitive intervention [3], regular physical exercise [4], and dietary intervention have shown some positive results for changes in cognitive function and biomarkers [5], additional evidence is needed for these interventions to be established as an AD prevention strategy. Furthermore, it is often difficult for MCI patients to perform preventive interventions with increased complexity and to maintain consistency for a significant period [6]. Therefore, the importance of an intervention that can be applied in a simple and fixed manner and maintained consistently for a certain period is emphasised.

In this regard, noninvasive brain stimulation has been proposed as a potential treatment option in the course of AD [7]. Transcranial direct current stimulation (tDCS), a type of noninvasive brain stimulation, modulates the excitability of cortical neurons depending on the current flow direction [8]. Moreover, tDCS has synaptic after-effects through long-term potentiation and alter oscillatory brain activity and functional connectivity patterns [9].

In some previous studies, AD patients showed improvement in the MMSE score [10], recognition memory [11], and global cognitive performance after tDCS was applied [12], while other studies found no significant difference in cognitive function compared with the sham group [13]. In these studies, the dorsolateral prefrontal cortex (DLPFC) has been most frequently targeted, and tDCS was applied in single or multiple sessions. There is a relative paucity of studies investigating the impact of tDCS on cognitive performance in patients with MCI. Prior research has shown an improvement in word retrieval performance after single-session anodal-tDCS application to the left ventral inferior frontal gyrus of patients with MCI [14]. However, another study found no significant difference in cognitive test battery scores after nine sessions of anodal-tDCS of the left DLPFC in patients with MCI [15].

Resting-state functional MRI (rs-fMRI) reveals intrinsic brain activity in the resting state and can approach functional segregation and integration by evaluating the fractional amplitude of low-frequency fluctuation (fALFF) and degree centrality (DC) [16]. Previous studies have shown that changes and disruptions in functional segregation and integration are associated with AD progression [17, 18]. Additionally, the default mode network (DMN) is a characteristic network of increased intrinsic brain activity during the resting state [19], and aberrant changes in this network have been demonstrated to reflect deterioration of AD [20]. Direct current stimulation has been documented to modulate the DMN and affect changes in functional segregation and integration parameters [20, 21]. However, few studies have evaluated the impact of tDCS on functional segregation and integration of intrinsic brain activity in the prodromal stage of AD.

Amyloid-beta ($A\beta$) retention and *APOE* $\epsilon 4$ genotype, which are representative factors affecting the progression and prognosis of AD, have been reported to affect the neuronal activity and cognitive decline significantly [22–25]. Furthermore, these AD risk factors have been demonstrated to affect the outcomes of preventive attempts in the prodromal stage of AD [26, 27]. Nevertheless, few studies have examined the effects of tDCS on cognitive and functional brain changes according to these AD risk factors in the MCI stage and there is little evidence for a precision medicine approach to the tDCS in the prodromal stage of AD.

Consequently, this study evaluated the impact of anodal-tDCS on cognitive performance and functional segregation and integration parameters in MCI patients, depending on $A\beta$ deposition and *APOE* $\epsilon 4$ -allele status. We hypothesised that the interaction between anodal-tDCS application and AD risk factors would affect changes in cognitive function and intrinsic brain activity in the prodromal stage of AD. Furthermore, we also expected that there would be a significant difference in changes in cognitive

function and intrinsic brain activity between MCI patients with and without AD risk factors after multiple sessions of anodal-tDCS.

Materials And Methods

Participants

Thirty-two MCI patients were recruited from the Brain Health Center, Yeoui-do St. Mary's Hospital, College of Medicine, The Catholic University of Korea, Republic of Korea, from May 2020 to December 2020. The study was conducted in accordance with the Declaration of Helsinki and was approved by the Institutional Review Board of the Catholic University of Korea. Informed and written consent was obtained from all participants.

The cognitive functions of all subjects were assessed with the Korean version of the Consortium to Establish a Registry for Alzheimer's Disease (CERAD-K) [28], which included a verbal fluency (VF) test, the 15-item Boston Naming Test (BNT), the Korean version of the Mini-Mental State Examination (MMSE-K) [29], word list memory (WLM), word list recall (WLR), word list recognition (WLRc), constructional praxis (CP), and constructional recall (CR) assessments. Additionally, total scores of memory domains (TM) were obtained by summing the CERAD-K, WLM, WLR, WLRc, and CR scores. Total CERAD-K scores were calculated by summing all CERAD-K subcategory scores, excluding the MMSE-K score.

Inclusion and exclusion criteria for MCI participants are described in the Supplementary Material. All subjects were evaluated at the Brain Health Center by an experienced psychiatrist and a psychologist. Details surrounding the usage of specific tests and the reviewing process are described in the Supplementary Material.

Experimental design

In this double-blind study, patients received 10 tDCS sessions (five times/week for 2 weeks: 10 sessions). The participants were assessed with the CERAD-K neuropsychological battery and underwent resting-state fMRI within 2 weeks before the first tDCS session and after the 10th session. Subjects also underwent [¹⁸F] flutemetamol (FMM) positron emission tomography–computed tomography (PET-CT) and *APOE* genotyping within 2 weeks before the first tDCS session.

tDCS application

A constant direct current (2 mA, 20 min) was administered by an MRI-compatible stimulator (YDS-301N, YBrain, Seoul, Republic of Korea). The anode was attached over the left DLPFC (F3 in the International 10/20 electroencephalogram system). The cathode was positioned over the right supraorbital region. The electrodes touched a water-soaked sponge (disc type, radius = 3 cm) placed on the scalp. For the subject to apply the device accurately, staff skilled in the use of the device visited the patient's residence for each stimulus session to guide device application.

fMRI data acquisition and data processing

Imaging data were collected by the Department of Radiology of Yeouido Saint Mary's Hospital at the Catholic University of Korea using a 3-T Siemens Skyra MRI machine and a 32-channel Siemens head coil (Siemens Medical Solutions, Erlangen, Germany). Parameters of structural and functional MRI data acquisition are described in the Supplementary Material.

We used the Data Processing Assistant for Resting-State fMRI (DPARSF) [30], which is based on Statistical Parametric Mapping (SPM, <http://www.fil.ion.ucl.ac.uk/spm>), to preprocess the fMR images. Slice timing and realignment for motion corrections were performed on the images. Subjects with excessive head motion (cumulative translation or rotation > 2 mm or 2°) were excluded. For spatial registration, T1-weighted images were co-registered to the mean rsfMRI image based on rigid-body transformation. For spatial normalisation, the International Consortium for Brain Mapping template was applied (resampling voxel size = 3 × 3 × 3 mm) and fitted to the "East Asian brain."

We further processed our functional data to fit them to fALFF and DC analysis with DPARSF. Linear trends were removed from the functional images, and data were filtered with a temporal band-pass of 0.01–0.08 Hz, to reduce low-frequency drift as well as physiological high-frequency respiratory and cardiac noise.

fALFF and DC analysis

To measure regional intrinsic brain activities in the resting state, fALFF was computed using individual preprocessed data [17]. The process of calculating fALFF is described in detail in the Supplementary Material. This fALFF calculation was repeated for each voxel in the whole brain to create a fALFF map for each participant, which was used in statistical analysis.

The DC was computed as the number of significant correlations (binarised) or as the sum of the weights of the significant connections (weighted) for each voxel. The map of the connectivity was then standardised by conversion to z scores, so that maps across participants could be averaged and compared. DC represents the most local and directly quantifiable centrality measure and has been widely used to examine node characteristics of intrinsic network connectivity [31]. Within the DMN, the DC value of a node indicates its connectivity strength to all the other nodes and reflects its importance in functional integration. Additionally, the fALFF and DC were calculated in 11 predefined regions-of-interest (ROIs) in the DMN and were used in statistical analysis (Table S1 in the Supplementary Material) [32]. Moreover, whole-brain voxel-wise analysis of fALFF and DC was also performed.

[¹⁸F] flutemetamol PET-CT image acquisition, assessments, and SUVR calculations

[¹⁸F] FMM was manufactured, and FMM-PET data were collected and analysed as described previously [33]. MRI of each participant was used to co-register and define the ROIs, and correct partial volume effects arising from the expansion of cerebrospinal spaces accompanying cerebral atrophy. We used a standardised uptake value ratio (SUVR) at 90-min post-injection to analyse the FMM PET data, using the pons ROI as the reference. Global A β burden was expressed as the average SUVR of the mean for the six cortical ROIs, including the frontal, superior parietal, lateral temporal, striatum, anterior, and posterior

cingulate cortex/precuneus ROIs. The PET scan was conducted within 4 weeks of clinical screening and cognitive function tests. We used a cut-off for “high” or ‘low’ neocortical SUVR of 0.62, consistent with cut-off values used in previous FMM PET study [33].

Statistical analysis

Statistical analyses for demographic data were performed using R software (version 2.15.3). Assumptions of normality were tested for continuous variables using the Kolmogorov–Smirnov test; all data demonstrated a normal distribution. Two sample *t*-tests and chi-square (χ^2) tests were used to probe for differences in demographic variables, clinical data, cognitive function, and fMRI measurements between MCI patients with and without A β deposition and the *APOE* ϵ 4-allele. Cognitive function and fMRI parameters (fALFF and DC in ROIs of the DMN) over 10 sessions were analysed for change with a repeated-measures analysis of variance (ANOVA) with time (pre-tDCS and post-tDCS) as repeated-measures factor and the presence of A β deposits and the *APOE* ϵ 4-allele as the between-subject factor, with adjustments for age, sex, and years of education. Multiple regression analysis was performed to evaluate the association between baseline [18 F] FMM SUVR_{PONS} and change in cognitive function and rs-fMRI measurements (fALFF and DC in ROIs of DMN), adjusting for age, sex, education years, and *APOE* ϵ 4-allele. Each variable was z-transformed using the mean and standard deviation. All statistical analyses used a two-tailed p-value < 0.05 to define statistical significance.

Additionally, to observe the effects of tDCS-by-group on fALFF and DC, a mixed analysis on a voxel-by-voxel basis, with groups (*APOE* ϵ 4-allele carrier vs. non-carrier; positive vs. negative for A β retention) as between-subject factors and tDCS (pre-tDCS vs. post-tDCS) as within-subject factors was performed on a brain mask. Age, sex, and years of education were included as covariates in the statistical tests. We designed a mixed analysis based on the SPM 12. An F-contrast was designed for the interaction effect analysis. Furthermore, paired *t*-tests were performed between pre-tDCS and post-tDCS on the individual z maps of fALFF and DC in each sub-group, respectively (negative or positive for A β retention; *APOE* ϵ 4-allele carrier or non-carrier). All statistical maps were corrected for multiple comparisons by Gaussian random field (GRF) correction combining the voxel *P* value < 0.001 and cluster level < 0.05 in DPABL_V5.1_201201 (<http://rfmri.org/dpabi>) [34].

Results

Baseline demographic and clinical data

Table 1 shows the baseline demographic and clinical data for MCI patients classified by the presence of A β deposits and the *APOE* ϵ 4-allele. MCI patients with A β deposits showed higher years of education than those without A β accumulation (Table 1A). The ratio of *APOE* ϵ 4 carriers was significantly higher in the group with A β deposits. This group displayed higher average SUVR_{PONS} than that without A β deposits (Table 1A).

There were no significant differences in age, sex, and years of education between patients with MCI with and without the *APOE* ϵ 4-allele (Table 1B). We found a higher ratio of A β deposits in *APOE* ϵ 4 carriers. *APOE* ϵ 4 carriers showed higher average $SUVR_{PONS}$ than non-carriers (Table 1B).

Neuropsychological performance

For the MMSE-K score, after adjustment for age, sex, and years of education, the main effect for the tDCS and A β deposits was not significant ($p = 0.278$; $p = 0.558$, respectively). However, there was a statistically significant trend toward an interaction between tDCS and A β deposition, possibly attributable to the increased MMSE-K score after tDCS application in patients with MCI without A β accumulation ($p = 0.055$, Fig. 1A). Additionally, we found a statistical trend for a negative association between baseline average $SUVR_{PONS}$ and changes in CERAD-K WLRc scores ($p = 0.071$, Fig. 1B).

Changes in functional segregation and integration of the DMN: an ROI-based analysis

In terms of functional segregation of the DMN, for temporal pole fALFF, the main effects of tDCS and A β deposits were not significant ($p = 0.584$; $p = 0.578$, respectively). However, there was a trend toward an interaction between tDCS and A β deposition, which might be attributed to increased temporal pole fALFF after tDCS application in MCI patients with A β deposits ($p = 0.071$, Fig. 2A). Additionally, we found a statistical trend toward a positive association between baseline average $SUVR_{PONS}$ and change in temporal pole fALFF, with adjustment for age, sex, years of education, and *APOE* genotype ($p = 0.090$, Fig. 2C). Additionally, the main effect of tDCS and *APOE* ϵ 4-allele was not significant ($p = 0.700$; $p = 0.117$, respectively). However, there was an interaction between tDCS and the *APOE* ϵ 4-allele, which could be attributed to increased temporal pole fALFF after tDCS application in MCI *APOE* ϵ 4-allele carriers ($p = 0.036$, Fig. 2B). Furthermore, we found a statistical trend toward an association between the baseline average $SUVR_{PONS}$ and change in temporal pole fALFF ($p = 0.090$, Fig. 2C).

With regard to functional integration of the DMN, for anterior medial prefrontal cortex (aMPFC) DC, the main effect of tDCS and *APOE* ϵ 4-allele was not significant ($p = 0.259$; $p = 0.257$, respectively). However, there was a statistical trend toward an interaction between tDCS and the *APOE* ϵ 4-allele, possibly attributable to increased aMPFC DC after tDCS application in MCI patients with A β deposits ($p = 0.056$, Fig. 2B). Additionally, we found a statistical trend toward a positive association between baseline average $SUVR_{PONS}$ and change in aMPFC DC ($p = 0.075$, Fig. 2C), but a negative association between average $SUVR_{PONS}$ and change in hippocampal formation DC ($p = 0.042$, Fig. 2C).

Changes in functional segregation and integration parameters: Whole brain voxel-based analysis

No brain regions showed a significant impact of tDCS-by-group interaction on the fALFF and DC in each sub-group. Brain regions that showed changes in fALFF after tDCS according to *APOE* genotype and A β deposition are displayed in Fig. 3A and B. The brain regions that showed significant changes in fALFF differed between MCI *APOE* ϵ 4 carriers and non-carriers. Additionally, increased and decreased fALFF values were observed in the right inferior temporal gyrus and crus I of the cerebellum, respectively, after tDCS, in both MCI patients with and without A β deposition. However, other brain regions that showed significant changes in fALFF also differed between MCI patients with and without A β deposits.

In terms of functional integration, brain regions that showed changes in DC after tDCS according to *APOE* genotype and A β deposition are shown in Fig. 4A and B. The brain regions that showed significant changes in DC differed between MCI *APOE4* carriers and non-carriers and patients with and without A β deposits. These anatomical regions, their corresponding MNI coordinates, and the intensity of peak points in each cluster are shown in Tables 2 and 3.

Discussion

The current study aimed to evaluate the impact of anodal-tDCS on cognitive performance and functional segregation and integration parameters in MCI patients, according to the presence of A β deposits and the *APOE* ϵ 4-allele. We evaluated the effect of interactions between anodal-tDCS application and AD risk factors on changes in cognitive function and intrinsic brain activity and explored differences in changes in cognitive function and spontaneous brain activity parameters between MCI patients with and without AD risk factors after multiple sequential anodal-tDCS sessions. With regard to cognitive performance, we found that there was a statistical trend toward an interaction between anodal-tDCS and A β deposition, which might be attributable to increased MMSE-K score after tDCS application in patients with MCI without A β accumulation. However, the impact of tDCS was not significant for changes in cognitive performance, including the MMSE-K score, in the current study.

Similarly, some prior studies have demonstrated improvement of semantic word-retrieval performance after a single-session anodal-tDCS application over the left ventral inferior frontal gyrus of MCI patients [14]. On the other hand, in another study that conducted a nine-session clinical trial for 3 weeks in MCI patients, there was no improvement in the objective neuropsychological test score [15]. In previous studies that performed anodal-tDCS on AD patients, they reported improved MMSE scores [10], recognition memory [11], and global functioning as compared to the sham group [12]. Additionally, in a meta-analysis of administering tDCS in patients with mild to moderate AD, repeated-session tDCS was not significantly more effective than single-session tDCS [35]. Moreover, stimulation of the temporal cortex significantly improved cognitive function, as compared to other areas, although the left DLPFC was the most frequently stimulated area [35]. The tDCS protocol of the present study did not contain factors that show beneficial effects identified in the meta-analysis, which could contribute to the restricted improvement in cognitive function. However, this meta-analysis targeted only seven studies, and the sample size was small, and thus results should be interpreted cautiously.

Additionally, although there have been no human studies on the effect of tDCS on cognitive functional changes according to A β deposits, an AD rat model, generated by injection of A β ₁₋₄₀ in the bilateral hippocampus, showed worse memory performance than control rats after repetitive anodal-tDCS [36]. We found a negative association between baseline A β accumulation and change in word recognition scores. A β deposits might inhibit cognitive improvement induced by tDCS, which modulates cortical excitability. However, given that this was only a statistical trend, it is necessary to conduct additional research with larger sample sizes.

With regard to changes in brain functional segregation parameters, this study found a statistical trend toward an interaction between tDCS and high AD risk factors, including the presence of A β deposits and the *APOE* ϵ 4-allele, in the left temporal pole. This interaction could contribute to increased temporal pole fALFF after anodal-tDCS application in MCI patients with A β deposition or the *APOE* ϵ 4-allele. The left temporal pole is part of the DMPFC subsystem of the DMN, which is vulnerable to AD pathology [32]. The DC of the left temporal lobe is lower in patients with MCI than in cognitively intact older adults [37]. Additionally, the temporal pole was associated with an abnormal insula network in MCI patients, and decreased functional connectivity in this network is related to cognitive decline in MCI patients [38]. Furthermore, the *APOE* ϵ 4-allele reduces connectivity of the hippocampal network, which includes the temporal pole in healthy older adults [24]. Although the present study showed a relative lack of evidence for functional integration changes, application of anodal-tDCS in prodromal AD patients with high-risk factors appears to restore the local intrinsic change in the temporal pole found in the MCI stage. This observation might support the hypothesis that tDCS-induced improvement is related to restoration, rather than compensation, of brain activity patterns [39].

In this study, the index reflecting the global functional integration of aMPFC also showed a similar pattern to the interaction found in the functional segregation parameter of the temporal pole. These results might be attributed to increased functional integration after anodal-tDCS application in MCI patients with the *APOE* ϵ 4 genotype. The aMPFC is an anterior core set of hubs in the DMN and shows global connectivity with other areas that constitute a DMN subsystem [32]. Additionally, the anterior DMN shows increased connectivity during AD and cognitive decline progression, and this change in the anterior hubs may be a compensatory response to AD pathology [40]. Furthermore, in the current study, the higher the baseline A β deposits level, the greater the changes in functional segregation parameters of the temporal pole and functional integration parameters of the aMPFC. These findings could support the concept of compensatory response to AD pathology after tDCS. However, it is possible that these results may underestimate A β -mediated hyperactivation in the early stages of AD [41]. Therefore, it is important to bear in mind the possible bias in these responses.

Another important finding was that a decreased change in DC of hippocampal formation was exhibited in the higher baseline A β deposits. This result might reflect decoupling of the hippocampal formation from posterior DMN nodes at the prodromal AD stage [42], and it is estimated that the tDCS application does not significantly affect pathologic functional changes in the hippocampal formation.

Lastly, in the present study, differences were observed in changing functional segregation and integration patterns after anodal-tDCS application, depending on the *APOE* ϵ 4-allele or A β deposits by whole-brain voxel-based analysis in MCI patients. In terms of functional segregation parameters after anodal-tDCS application, our MCI patients with *APOE* ϵ 4-allele displayed increased local intrinsic brain activity in DMN hub regions and AD compensatory regions, in which previous studies have shown a decreasing trend of fALFF across the AD spectrum [43]. However, MCI patients without the *APOE* ϵ 4-allele showed increased fALFF after repetitive anodal-tDCS administration in different brain regions, such as the inferior occipital gyrus, calcarine fissure, and surrounding cortex. The inferior occipital gyrus has been documented to be

vulnerable during the MCI stage and is connected with deep brain structures related to MCI pathology [44]. Additionally, the fALFF of the calcarine fissure and surrounding cortex showed a decreasing trend during the AD course [45]. However, the lack of information on the *APOE* genotype in previous reports adds further caution regarding the interpretation of these findings. In MCI patients in the present study, regional intrinsic activity of the inferior temporal gyrus was increased both with and without A β deposits, and this region has shown lower local integrity in the MCI group than in the normal group in our previous study [46]. Furthermore, the cerebellum, in which regional intrinsic brain activity increased after tDCS in MCI patients with A β deposits, was also the area in which fALFF tended to decrease with AD progression in a previous study [43]. Therefore, these findings might indicate that increased fALFF in functionally deteriorated regions might be induced by sequential anodal-tDCS during the prodromal AD stage. Additionally, MCI patients without A β deposits showed increased intrinsic brain activity at various locations in the frontal gyrus, unlike those with A β deposition after multiple sessions of anodal-tDCS. In a prior study, the frontal cortex showed hypermetabolism in MCI patients without A β accumulation, and MCI patients with cortical hypermetabolism did not convert to AD during the follow-up period [47]. Hence, it could conceivably be hypothesised that sequential anodal-tDCS may restore spontaneous brain activity in MCI patients with A β deposits but play a compensatory role in those without A β deposition. Future studies on the current topic are therefore recommended.

Regarding the functional integration parameter evaluated by whole-brain voxel-based analysis, we found that MCI patients with AD risk factors showed increased DC in the cerebellum after anodal-tDCS, similar to the pattern of functional segregation parameter changes. Another finding was that MCI patients with the *APOE* ϵ 4-allele showed increased temporal pole DC after anodal-tDCS, in which a fALFF increase was observed in ROI-based analysis. According to these data, it might be assumed that the intensity at which a region locally activated by anodal-tDCS is integrated with other regions increases simultaneously in MCI patients with high-risk factors of AD.

A significant limitation of the current study is that the sample size was relatively small, and no comparisons with a sham group were made. Consequently, there is a relative lack of statistical robustness for the interaction between anodal-tDCS application and AD risk factors for changes in cognitive function and brain functional segregation and integration. Lastly, considering the after-effects of tDCS [9] and the important role of stimulation frequency for outcomes in MCI and AD patients [48], further research, applying tDCS for a longer duration, is needed.

Conclusion

This study provides an initial step in searching for conditions that may deliver optimal effects when tDCS is administered during the AD prodromal stage. It is necessary to identify the preventive and therapeutic mechanisms of tDCS in AD more clearly, and to establish a foundation for precision medicine for tDCS treatment of AD.

Abbreviations

A β , amyloid-beta

AD, Alzheimer's disease

BNT, Boston Naming Test

CERAD-K, Korean version of the Consortium to Establish a Registry for Alzheimer's Disease

CP, constructional praxis

CR, constructional recall

DC, degree centrality

DLPFC, dorsolateral prefrontal cortex

DMN, default mode network

DPARF, Data Processing Assistant for Resting-State

fALFF, fractional amplitude of low-frequency fluctuation

fMRI, functional magnetic resonance imaging

FMM, [^{18}F] flutemetamol

MCI, mild cognitive impairment

MMSE, Mini-Mental State Examination

PET-CT, positron emission tomography-computed tomography

SD, standard deviation

SUV_R, standardized uptake value ratio

tDCS, transcranial direct current stimulation

TM, total scores of memory domains

VF, verbal fluency

WLM, word list memory

WLR, word list recall

WLR_c, word list recognition

Declarations

Ethics approval and consent to participate

The study was conducted in accordance with the ethical and safety guidelines set forth by the Institutional Review Board of the Catholic University of Korea. The Institutional Review Board of the Catholic University of Korea approved all study procedures, and informed consent was obtained from all participants and their guardians.

Consent for publication

Not applicable.

Availability of data and materials

The datasets generated or analysed during the current study are not publicly available due to Patient Data Management Protocol of Yeouido St. Mary's Hospital but are available from the corresponding author on reasonable request.

Competing interests

The authors declare that they have no competing interests.

Funding

This work was supported by a National Research Foundation of Korea (NRF) grant funded by the Korean government (Ministry of Science and ICT) (No. 2019R1A2C2009100 and 2019R1C1C1007608). The funders had no role in study design, data collection and analysis, decision to publish, or preparation of the manuscript.

Authors' contributions

Dong Woo Kang: Conceptualisation, Methodology, Data Curation, Writing - Original Draft, Visualisation, Formal analysis, Funding acquisition. **Sheng-Min Wang:** Methodology, Data Curation, Writing - Review & Editing. **TaeYeong Kim:** Software, Investigation. **Donghyeon Kim:** Software, Investigation. **Hae-Ran Na:** Investigation, Visualization. **Nak-Young Kim:** Methodology, Data Curation. **Chang Uk Lee:** Conceptualisation, Supervision. **Hyun Kook Lim:** Conceptualisation, Methodology, Writing - Review & Editing, Supervision, Project administration, Funding acquisition.

Acknowledgments

We would like to thank Editage (www.editage.co.kr) for English language editing.

References

1. Petersen RC, Negash S. Mild cognitive impairment: an overview. *CNS spectrums*. 2008;13(1):45.
2. Gauthier S, Reisberg B, Zaudig M, Petersen RC, Ritchie K, Broich K, et al. Mild cognitive impairment. *The lancet*. 2006;367(9518):1262-70.
3. Jean L, Bergeron M-È, Thivierge S, Simard M. Cognitive intervention programs for individuals with mild cognitive impairment: systematic review of the literature. *The American Journal of Geriatric Psychiatry*. 2010;18(4):281-96.
4. Lautenschlager NT, Cox K, Kurz AF. Physical activity and mild cognitive impairment and Alzheimer's disease. *Current neurology and neuroscience reports*. 2010;10(5):352-8.
5. Singh B, Parsaik AK, Mielke MM, Erwin PJ, Knopman DS, Petersen RC, et al. Association of mediterranean diet with mild cognitive impairment and Alzheimer's disease: a systematic review and meta-analysis. *Journal of Alzheimer's disease*. 2014;39(2):271-82.
6. Coley N, Ngandu T, Lehtisalo J, Soininen H, Vellas B, Richard E, et al. Adherence to multidomain interventions for dementia prevention: data from the FINGER and MAPT trials. *Alzheimer's & Dementia*. 2019;15(6):729-41.
7. Liu CS, Rau A, Gallagher D, Rajji TK, Lanctôt KL, Herrmann N. Using transcranial direct current stimulation to treat symptoms in mild cognitive impairment and Alzheimer's disease. *Neurodegenerative disease management*. 2017;7(5):317-29.
8. Nitsche MA, Fricke K, Henschke U, Schlitterlau A, Liebetanz D, Lang N, et al. Pharmacological modulation of cortical excitability shifts induced by transcranial direct current stimulation in humans. *The Journal of physiology*. 2003;553(1):293-301.
9. Hansen N. Action mechanisms of transcranial direct current stimulation in Alzheimer's disease and memory loss. *Frontiers in psychiatry*. 2012;3:48.
10. Ferrucci R, Mameli F, Guidi I, Mrakic-Sposta S, Vergari M, Marceglia S, et al. Transcranial direct current stimulation improves recognition memory in Alzheimer disease. *Neurology*. 2008;71(7):493-8.
11. Boggio PS, Khoury LP, Martins DC, Martins OE, De Macedo E, Fregni F. Temporal cortex direct current stimulation enhances performance on a visual recognition memory task in Alzheimer disease. *Journal of Neurology, Neurosurgery & Psychiatry*. 2009;80(4):444-7.
12. Khedr EM, Gamal NFE, El-Fetoh NA, Khalifa H, Ahmed EM, Ali AM, et al. A double-blind randomised clinical trial on the efficacy of cortical direct current stimulation for the treatment of Alzheimer's disease. *Frontiers in aging neuroscience*. 2014;6:275.
13. Bystad M, Grønli O, Rasmussen ID, Gundersen N, Nordvang L, Wang-Iversen H, et al. Transcranial direct current stimulation as a memory enhancer in patients with Alzheimer's disease: a randomised, placebo-controlled trial. *Alzheimer's research & therapy*. 2016;8(1):1-7.
14. Meinzer M, Lindenberg R, Phan MT, Ulm L, Volk C, Flöel A. Transcranial direct current stimulation in mild cognitive impairment: behavioral effects and neural mechanisms. *Alzheimer's & Dementia*. 2015;11(9):1032-40.
15. Yun K, Song I-U, Chung Y-A. Changes in cerebral glucose metabolism after 3 weeks of noninvasive electrical stimulation of mild cognitive impairment patients. *Alzheimer's research & therapy*.

- 2016;8(1):1-9.
16. Sporns O. Network attributes for segregation and integration in the human brain. *Current opinion in neurobiology*. 2013;23(2):162-71.
 17. Zou Q-H, Zhu C-Z, Yang Y, Zuo X-N, Long X-Y, Cao Q-J, et al. An improved approach to detection of amplitude of low-frequency fluctuation (ALFF) for resting-state fMRI: fractional ALFF. *Journal of neuroscience methods*. 2008;172(1):137-41.
 18. Guo Z, Liu X, Hou H, Wei F, Liu J, Chen X. Abnormal degree centrality in Alzheimer's disease patients with depression: A resting-state functional magnetic resonance imaging study. *Experimental gerontology*. 2016;79:61-6.
 19. Buckner RL, Andrews-Hanna JR, Schacter DL. The brain's default network: anatomy, function, and relevance to disease. 2008.
 20. Binnewijzend MA, Schoonheim MM, Sanz-Arigita E, Wink AM, van der Flier WM, Tolboom N, et al. Resting-state fMRI changes in Alzheimer's disease and mild cognitive impairment. *Neurobiology of aging*. 2012;33(9):2018-28.
 21. Zeng M, Wang L, Cheng B, Qi G, He J, Xu Z, et al. Transcutaneous spinal cord direct current stimulation modulates functional activity and integration in idiopathic restless legs syndrome. *Frontiers in Neuroscience*. 2020;14:873.
 22. Hedden T, Van Dijk KR, Becker JA, Mehta A, Sperling RA, Johnson KA, et al. Disruption of functional connectivity in clinically normal older adults harboring amyloid burden. *Journal of Neuroscience*. 2009;29(40):12686-94.
 23. Lim YY, Ellis KA, Pietrzak RH, Ames D, Darby D, Harrington K, et al. Stronger effect of amyloid load than APOE genotype on cognitive decline in healthy older adults. *Neurology*. 2012;79(16):1645-52.
 24. Trachtenberg AJ, Filippini N, Ebmeier KP, Smith SM, Karpe F, Mackay CE. The effects of APOE on the functional architecture of the resting brain. *Neuroimage*. 2012;59(1):565-72.
 25. Christensen H, Batterham PJ, Mackinnon AJ, Jorm AF, Mack HA, Mather KA, et al. The association of APOE genotype and cognitive decline in interaction with risk factors in a 65–69 year old community sample. *BMC geriatrics*. 2008;8(1):1-10.
 26. Kemppainen N, Johansson J, Teuho J, Parkkola R, Joutsa J, Ngandu T, et al. Brain amyloid load and its associations with cognition and vascular risk factors in FINGER Study. *Neurology*. 2018;90(3):e206-e13.
 27. Berkowitz C, Mosconi L, Rahman A, Scheyer O, Hristov H, Isaacson RS. Clinical application of APOE in Alzheimer's prevention: A precision medicine approach. *The journal of prevention of Alzheimer's disease*. 2018;5(4):245-52.
 28. Lee JH, Lee KU, Lee DY, Kim KW, Jhoo JH, Kim JH, et al. Development of the Korean Version of the Consortium to Establish a Registry for Alzheimer's Disease Assessment Packet (CERAD-K) clinical and neuropsychological assessment batteries. *The Journals of Gerontology Series B: Psychological Sciences and Social Sciences*. 2002;57(1):P47-P53.

29. Park J-H. Standardisation of Korean version of the Mini-Mental State Examination (MMSE-K) for use in the elderly. Part II. Diagnostic validity. *J Korean Neuropsychiatr Assoc.* 1989;28:508-13.
30. Yan C, Zang Y. DPARSF: a MATLAB toolbox for "pipeline" data analysis of resting-state fMRI. *Frontiers in systems neuroscience.* 2010;4:13.
31. Zuo X-N, Ehmke R, Mennes M, Imperati D, Castellanos FX, Sporns O, et al. Network centrality in the human functional connectome. *Cerebral cortex.* 2012;22(8):1862-75.
32. Andrews-Hanna JR, Reidler JS, Sepulcre J, Poulin R, Buckner RL. Functional-anatomic fractionation of the brain's default network. *Neuron.* 2010;65(4):550-62.
33. Thurfjell L, Lilja J, Lundqvist R, Buckley C, Smith A, Vandenberghe R, et al. Automated quantification of 18F-flutemetamol PET activity for categorising scans as negative or positive for brain amyloid: concordance with visual image reads. *Journal of Nuclear Medicine.* 2014;55(10):1623-8.
34. Bansal R, Peterson BS. Cluster-level statistical inference in fMRI datasets: the unexpected behavior of random fields in high dimensions. *Magnetic resonance imaging.* 2018;49:101-15.
35. Cai M, Guo Z, Xing G, Peng H, Zhou L, Chen H, et al. Transcranial Direct Current Stimulation Improves Cognitive Function in Mild to Moderate Alzheimer Disease. *Alzheimer Disease & Associated Disorders.* 2019;33(2):170-8.
36. Yang W-J, Wen H-Z, Zhou L-X, Luo Y-P, Hou W-S, Wang X, et al. After-effects of repetitive anodal transcranial direct current stimulation on learning and memory in a rat model of Alzheimer's disease. *Neurobiology of learning and memory.* 2019;161:37-45.
37. Jacini F, Sorrentino P, Lardone A, Rucco R, Baseliçe F, Cavaliere C, et al. Amnestic mild cognitive impairment is associated with frequency-specific brain network alterations in temporal poles. *Frontiers in aging neuroscience.* 2018;10:400.
38. Xie C, Bai F, Yu H, Shi Y, Yuan Y, Chen G, et al. Abnormal insula functional network is associated with episodic memory decline in amnestic mild cognitive impairment. *Neuroimage.* 2012;63(1):320-7.
39. Nyberg L, Lövdén M, Riklund K, Lindenberger U, Bäckman L. Memory aging and brain maintenance. *Trends in cognitive sciences.* 2012;16(5):292-305.
40. Jones DT, Machulda MM, Vemuri P, McDade E, Zeng G, Senjem M, et al. Age-related changes in the default mode network are more advanced in Alzheimer disease. *Neurology.* 2011;77(16):1524-31.
41. Zott B, Simon MM, Hong W, Unger F, Chen-Engerer H-J, Frosch MP, et al. A vicious cycle of β amyloid-dependent neuronal hyperactivation. *Science.* 2019;365(6453):559-65.
42. Dillen KN, Jacobs HI, Kukolja J, Richter N, von Reutern B, Onur ÖA, et al. Functional disintegration of the default mode network in prodromal Alzheimer's disease. *Journal of Alzheimer's disease.* 2017;59(1):169-87.
43. Yang L, Yan Y, Wang Y, Hu X, Lu J, Chan P, et al. Gradual disturbances of the amplitude of low-frequency fluctuations (ALFF) and fractional ALFF in Alzheimer spectrum. *Frontiers in neuroscience.* 2018;12:975.

44. Liu J, Zhang B, Wilson G, Kong J, Weiner MW, Aisen P, et al. New Perspective for Noninvasive Brain Stimulation Site Selection in Mild Cognitive Impairment: Based on Meta-and Functional Connectivity Analyses. *Frontiers in aging neuroscience*. 2019;11:228.
45. Yang L, Yan Y, Li Y, Hu X, Lu J, Chan P, et al. Frequency-dependent changes in fractional amplitude of low-frequency oscillations in Alzheimer's disease: a resting-state fMRI study. *Brain imaging and behavior*. 2019:1-15.
46. Kang DW, Lim HK, Joo S-H, Lee NR, Lee C-U. Alterations in intra-and interregional intrinsic brain connectivity are differentially associated with memory performance in amnesic mild cognitive impairment. *Dementia and geriatric cognitive disorders*. 2018;46(3-4):229-42.
47. Ashraf A, Fan Z, Brooks D, Edison P. Cortical hypermetabolism in MCI subjects: a compensatory mechanism? *European journal of nuclear medicine and molecular imaging*. 2015;42(3):447-58.
48. Batsikadze G, Moliadze V, Paulus W, Kuo MF, Nitsche M. Partially non-linear stimulation intensity-dependent effects of direct current stimulation on motor cortex excitability in humans. *The Journal of physiology*. 2013;591(7):1987-2000.

Tables

Table 1 Demographic and clinical characteristics of study participants categorised by (A) Ab deposits and (B) *APOE* e4 allele

(A)

Ab deposits	Ab-negative (N = 10)	Ab-positive (N = 22)	<i>p</i>
Age	77.5 ± 6.1	72.3 ± 7.1	0.054
Sex			> 0.999
- Male	4 (40.0%)	9 (40.9%)	
- Female	6 (60.0%)	13 (59.1%)	
Years of education	9.6 ± 4.4	13.5 ± 4.9	0.039
<i>APOE</i> e4 allele			0.001
- Non-carrier	9 (90.0%)	4 (18.2%)	
- Carrier	1 (10.0%)	18 (81.8%)	
Average SUVR _{PONS} of [¹⁸ F] flutemetamol	0.5 ± 0.1	0.7 ± 0.1	< 0.001

(B)

<i>APOE</i> e4 allele	Non-carrier (N = 13)	Carrier (N = 19)	<i>p</i>
Age (years)	75.8 ± 6.4	72.6 ± 7.6	0.229
Sex			0.873
- Male	6 (46.2%)	7 (36.8%)	
- Female	7 (53.8%)	12 (63.2%)	
Years of education	11.1 ± 4.2	13.1 ± 5.5	0.268
Ab deposits			0.001
- Ab neg	9 (69.2%)	1 (5.3%)	
- Ab pos	4 (30.8%)	18 (94.7%)	
Average SUVR _{PONS} of [¹⁸ F] flutemetamol	0.6 ± 0.2	0.7 ± 0.1	0.003

Data are presented as the mean ± SD unless indicated otherwise. Ab Neg, negative deposits of Ab; Ab pos, positive deposits of Ab; SUVR_{PONS}, standardised uptake value ratios of [¹⁸F] flutemetamol, using pons as a reference region.

Table 2 Changes in fALFF of MCI patients after tDCS, according to (A) *APOE* genotype and (B) Ab deposits
(A)

Region	L/R	Cluster	Peak T value	Peak MNI coordinates (x, y, z)		
Changes in fALFF of MCI <i>APOE</i> e4 carriers						
tDCS > baseline						
Middle temporal gyrus	R	98	3.9585	51	-3	-24
Lobule III of cerebellum	L	187	5.0774	-3	-45	-21
Parahippocampal gyrus	R	40	3.2239	33	-18	-30
Precuneus	L	41	4.831	-18	-48	3
Inferior frontal gyrus, triangular part	L	81	3.4026	-45	30	24
Middle cingulate gyri	R	62	3.8016	6	12	36
Midcingulate area	L	189	3.1684	-12	-42	51
tDCS < baseline						
Middle occipital gyrus	R	45	-5.1376	27	-75	30
Superior frontal gyrus	L	384	-5.2261	-30	-3	69
Superior parietal gyrus	R	250	-4.3472	27	-51	72
Postcentral gyrus	L	38	-4.5553	-42	-21	57
Supplementary motor area	R	43	-3.7324	3	18	63
Superior frontal gyrus	R	61	-4.9716	15	-9	69
Changes in fALFF of MCI <i>APOE</i> e4 non-carriers						
tDCS > baseline						
Inferior occipital gyrus	L	29	5.1353	-42	-72	-6
Calcarine fissure and surrounding cortex	R	29	3.8547	18	-81	9
tDCS < baseline						
Superior frontal gyrus, orbital	L	47	-4.0932	-27	57	-3
Supplementary motor area	L	79	-4.4351	-3	15	63

(B)

Region	L/R	Cluster	Peak T value	Peak MNI coordinates (x, y, z)		
Changes in fALFF of MCI patients with Ab deposits						
tDCS > baseline						
Inferior temporal gyrus	R	61	4.0777	39	-6	-45
Crus I of of cerebellum	L	36	4.6073	-15	-72	-33
Lobule III of cerebellum	L	62	4.374	-3	-45	-21
tDCS < baseline						
Crus I of of cerebellum	R	40	-4.5424	36	-81	-36
Supramarginal gyrus	R	38	-3.4884	60	-30	33
Superior parietal gyrus	R	99	-4.3392	27	-51	72
Superior frontal gyrus, medial	R	146	-3.5363	9	33	57
Superior frontal gyrus	L	119	-4.3879	-27	-9	72
Paracentral lobule	L	35	-2.7845	-6	-30	78
Changes in fALFF of MCI patients without Ab deposits						
tDCS > baseline						
Inferior temporal gyrus	R	29	4.9944	48	-21	-27
Middle temporal gyrus	L	28	6.7989	-57	-36	-6
Middle frontal gyrus	L	42	6.345	-39	45	-9
Inferior frontal gyrus, triangular part	L	32	5.266	-42	18	6
Superior frontal gyrus, medial	L	27	7.7112	-9	63	21
Precuneus	R	32	4.4101	9	-60	54
tDCS < baseline						
Crus I of cerebellum	R	27	-4.3276	48	-54	-27
Cuneus	L	36	-4.2645	-6	-81	24
Superior occipital gyrus	R	30	-4.1793	24	-90	27
Middle frontal gyrus	R	29	-5.2138	45	12	42
Supplementary motor area	R	27	-6.8382	6	15	63
Postcentral gyrus	L	28	-3.587	-24	-27	72

Whole-brain voxel-wise fALFF analysis results. Thresholds were set using GRF correction at a p value of $< .05$, voxel $p < .001$. The statistical threshold of the cluster size is described in Figure 3.

Abbreviations: MNI, Montreal Neurological Institute coordinate; aMCI, amnesic mild cognitive impairment group; L/R, left/right; tDCS, transcranial direct current stimulation; fALFF, fractional amplitude of low-frequency fluctuation.

Table 3 Changes in DC of MCI patients after tDCS, according to (A) *APOE* genotype and (B) Ab deposits

(A)

Region	L/R	Cluster	Peak T value	Peak MNI coordinates (x, y, z)		
Changes in DC of MCI patients with <i>APOE</i> e4 carrier						
tDCS > baseline						
Lobule VIIB of cerebellar hemisphere	R	78	3.7442	30	-72	-48
Temporal pole: superior temporal gyrus	R	115	4.3302	45	3	-15
Temporal pole: superior temporal gyrus	L	108	4.3954	-42	3	-15
Calcarine fissure and surrounding cortex	R	67	3.7306	9	-87	9
tDCS < baseline						
Superior parietal gyrus	R	178	-4.1919	27	-63	51
Superior parietal gyrus	L	767	-5.1001	-24	-69	48
Changes in DC of MCI patients with <i>APOE</i> e4 non-carrier						
tDCS > baseline						
Inferior temporal gyrus	L	48	4.5971	-42	-60	-6
Middle occipital gyrus	R	60	4.2846	33	-78	30
Middle occipital gyrus	L	84	4.7948	-15	-81	39
tDCS < baseline						
Superior frontal gyrus, medial	L	338	-6.6552	0	57	0

(B)

Region	L/R	Cluster	Peak T value	Peak MNI coordinates (x, y, z)		
Changes in DC of MCI patients with Ab deposits						
tDCS > baseline						
Lobule VIII of cerebellum	R	70	3.9953	12	-66	-45
Calcarine fissure and surrounding cortex	R	230	4.6267	9	-87	9
tDCS < baseline						
Superior parietal gyrus	L	76	-3.427	-21	-51	45
Changes in DC of MCI patients without Ab deposits						
tDCS > baseline						
Superior frontal gyrus, medial orbital	R	53	4.7797	12	66	-9
Middle frontal gyrus	L	70	4.8997	-48	42	15
Middle temporal gyrus	R	53	4.9548	66	-48	9
tDCS < baseline						
Lingual gyrus	R	55	-5.8024	12	-81	-12
Superior frontal gyrus, medial	L	48	-4.093	0	57	0
Lenticular nucleus, Putamen	L	48	-4.2643	-18	3	6
Middle occipital gyrus	L	50	-3.9537	-24	-84	9
Supplementary motor area	R	115	-3.9209	12	12	69
Precentral gyrus	L	59	-3.5792	-33	-21	72
Postcentral gyrus	R	153	-5.5196	27	-30	60

Whole-brain voxel-wise DC analysis results Thresholds were set using GRF correction at a p value of < .05, voxel p < .001. The statistical threshold of the cluster size is described in Figure 3.

Abbreviations: MNI, Montreal Neurological Institute coordinate; aMCI, amnesic mild cognitive impairment group; L/R, left/right; tDCS, transcranial direct current stimulation; fALFF, fractional amplitude of low-frequency fluctuation.

Figures

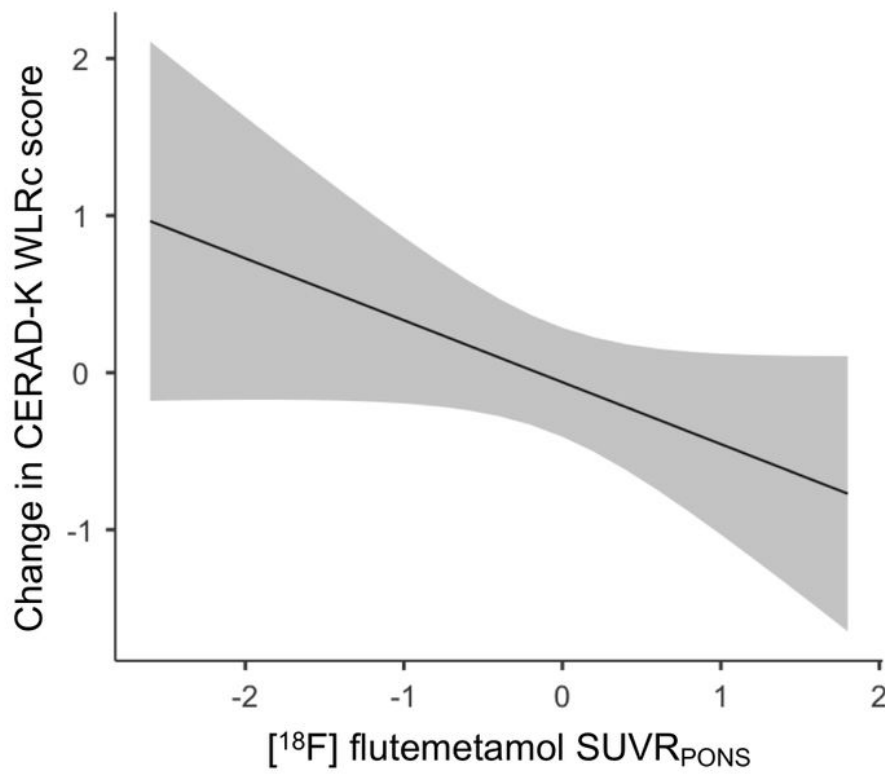
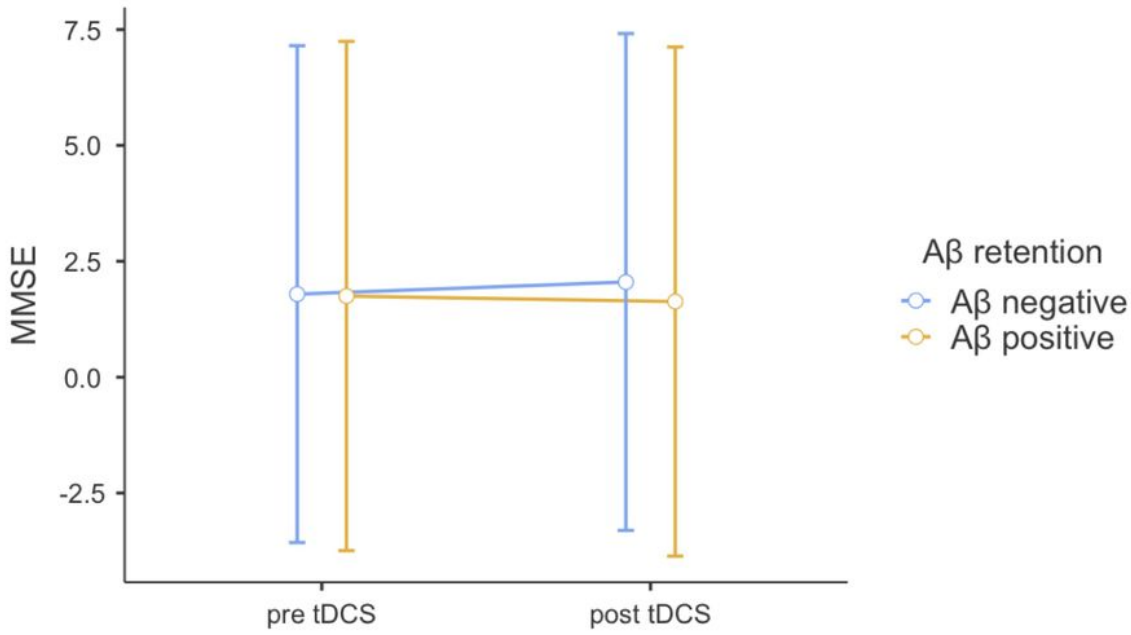


Figure 1

(A) Impact of interaction between tDCS and Ab deposits on cognitive functions, (B) Associations between [18F] flutemetamol SUVRPONS and changes in cognitive function test score before and after tDCS

Repeated-measures analysis of variance was used to predict the impact of interaction between tDCS and Ab deposits on cognitive functions, adjusting for age, sex, and education years ($p = 0.055$). Multiple linear regression analysis was used to evaluate the associations between [18F] flutemetamol SUVRPONS and changes in cognitive function test scores before and after tDCS, with adjustments for age, sex, and education years ($p = 0.071$). Each variable was z-transformed using the mean and standard deviation. Changes in cognitive function test scores were defined as post-tDCS z-transformed scores minus pre-tDCS z-transformed scores. Abbreviations: tDCS, transcranial direct current stimulation; SUVR, standardised uptake value ratio; Ab, amyloid beta; MMSE, Mini-Mental State Examination; CERAD-K, the Korean version of the Consortium to Establish a Registry for Alzheimer's Disease; WLRc, word list recognition

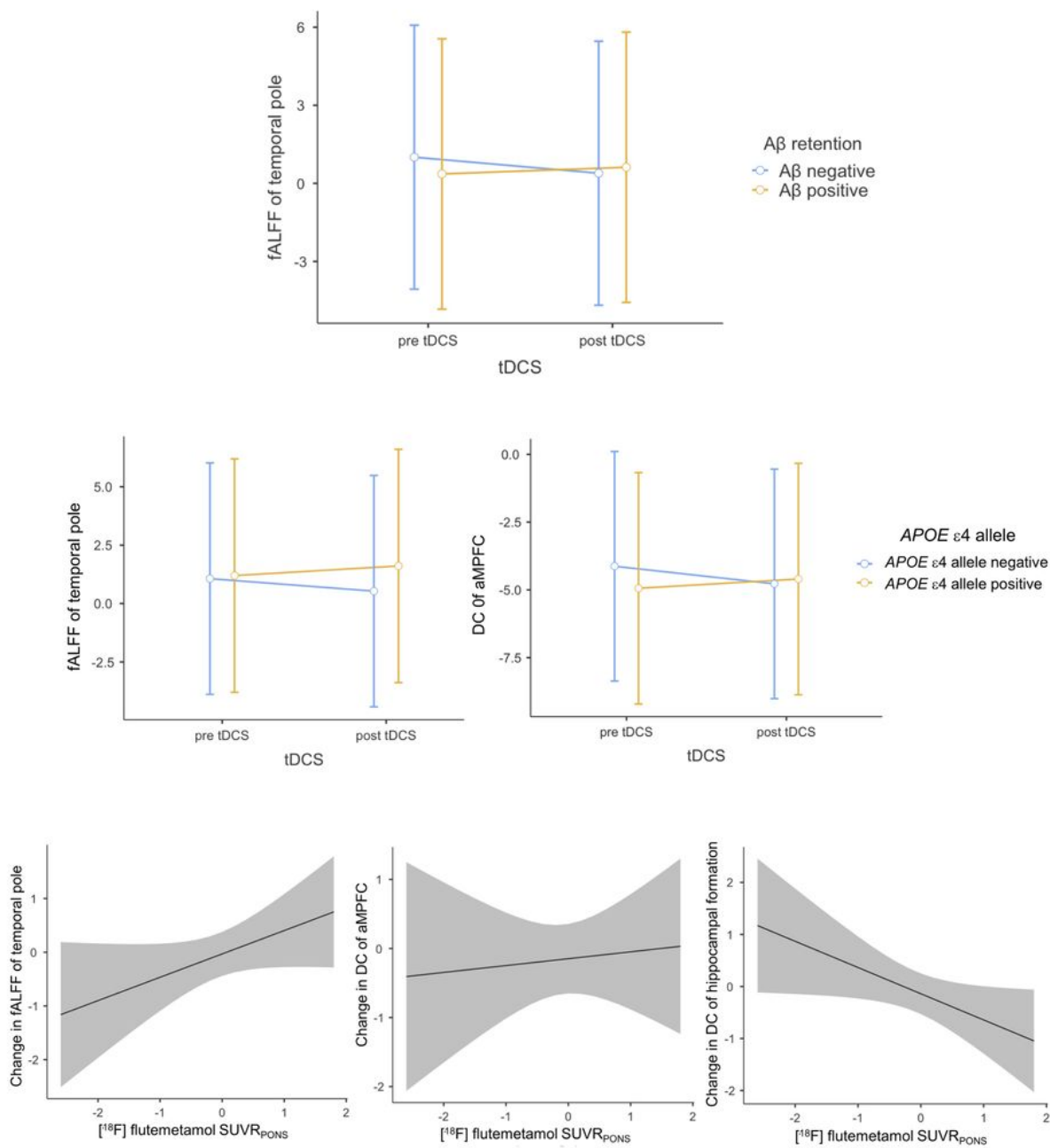


Figure 2

(A) Impact of interaction between tDCS and Ab deposits on fALFF and (B) between tDCS and APOE e4 allele on fALFF and DC. (C) Associations between [18F] flutemetamol SUVR_{PONS} and changes in amplitude of fALFF and DC. Repeated-measures analysis of variance was used to predict the impact of interaction (A) between tDCS and Ab deposits on fALFF, with adjustment for age, sex, and education years ($p = 0.071$), and (B) the impact of interaction between tDCS and APOE e4 allele on fALFF and DC,

with adjustment for age, sex, and education years ($p = 0.036$; $p = 0.056$, respectively). (C) Multiple linear regression analysis was used to evaluate the associations between [18F] flutemetamol SUVRPONS and changes in fALFF and DC before and after tDCS, with adjustment for age, sex, and education years ($p = 0.090$; $p = 0.075$; $p = 0.042$). Each variable was z-transformed using the mean and standard deviation. Changes in fALFF and DC were defined as post-tDCS z-transformed values minus pre-tDCS z-transformed values. Abbreviations: tDCS, transcranial direct current stimulation; fALFF, fractional amplitude of low-frequency fluctuation; DC, degree centrality; SUVR, standardised uptake value ratio; Ab, amyloid beta; aMPFC, anterior medial prefrontal cortex

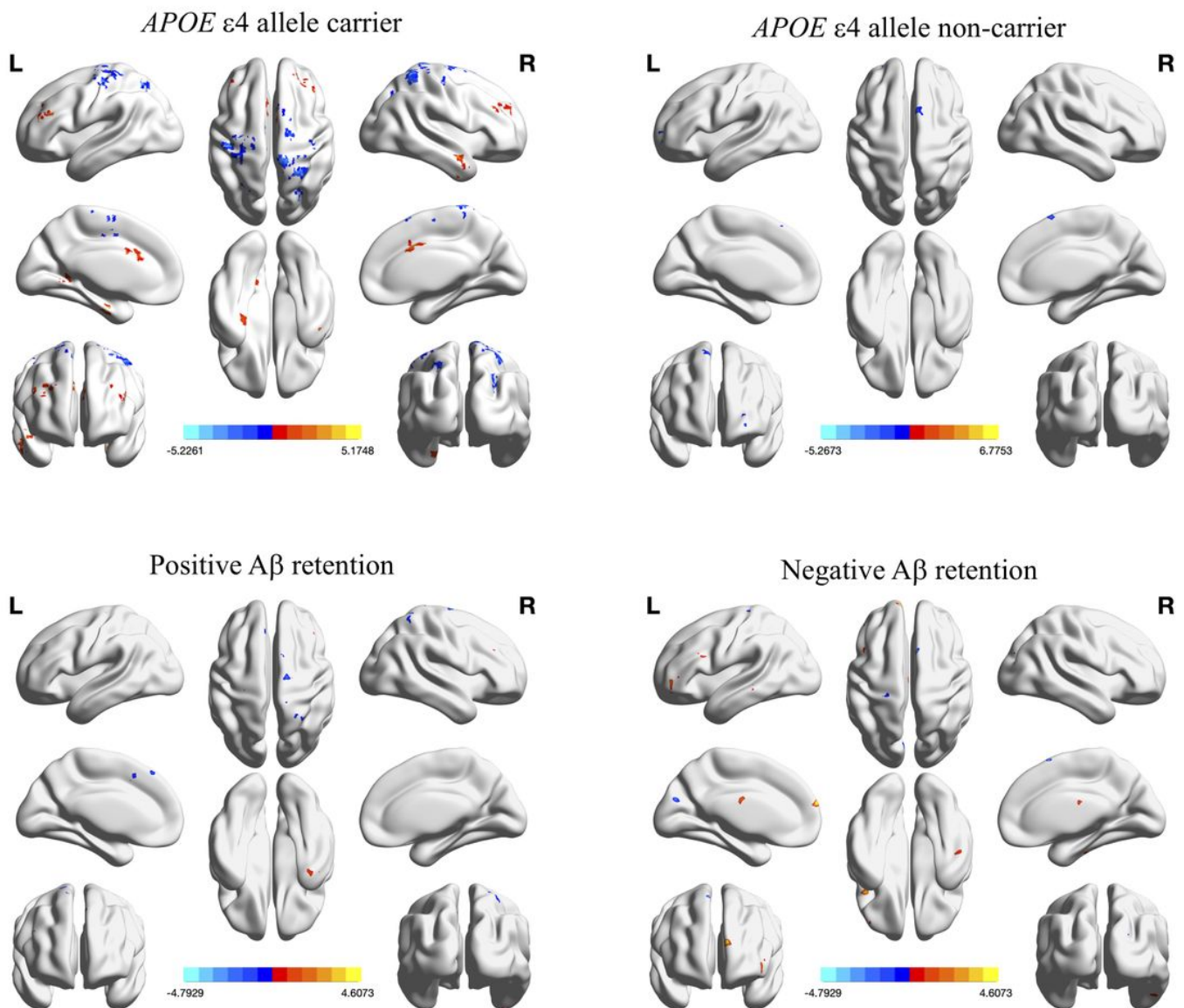


Figure 3

Significant changes in fALFF after tDCS for patients with mild cognitive impairment (A) with and without the APOE e4 allele, and (B) with and without Ab deposits Whole-brain voxel-wise fALFF analysis results. Thresholds were set using GRF correction at a p value of < .05, voxel p < .001. (A) APOE e4 allele carrier, cluster size > 38; APOE e4 allele non-carrier, cluster size > 29; (B) Ab deposit-positive, cluster size > 35; Ab deposit-negative, cluster size > 27. Brain regions that showed significant changes are described in Table 2. Abbreviations: tDCS, transcranial direct current stimulation; fALFF, fractional amplitude of low-frequency fluctuation; Ab, amyloid beta

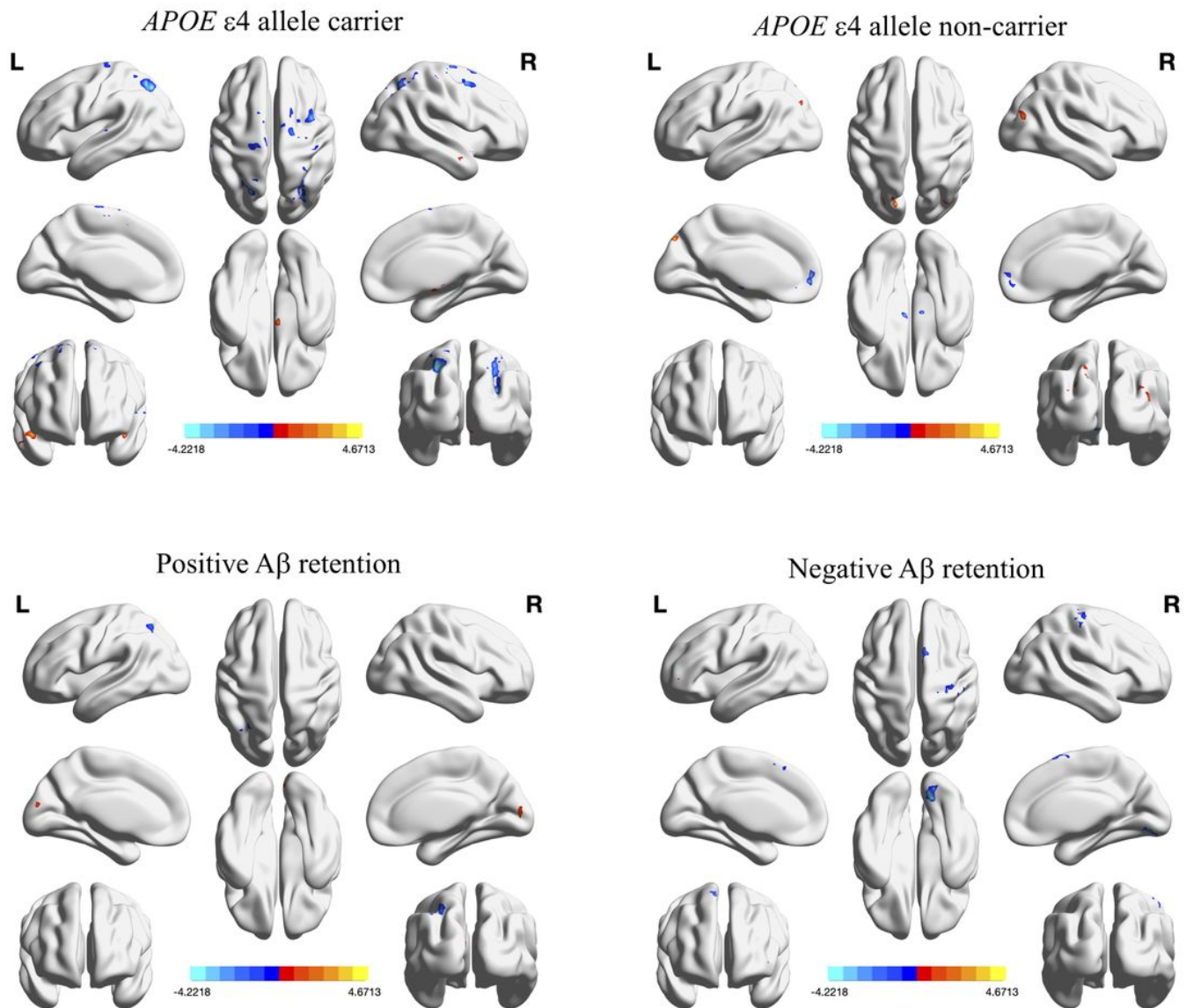


Figure 4

Significant changes in DC after tDCS of mild cognitive impairment patients (A) with and without the APOE e4 allele, and (B) with and without Ab deposits Whole-brain voxel-wise DC analysis results.

Thresholds were set using GRF correction at a p value of $< .05$, voxel $p < .001$. (A) APOE e4 allele carrier, cluster size > 62 ; APOE e4 allele non-carrier, cluster size > 48 ; (B) Ab deposit-positive, cluster size > 52 ; Ab deposit-negative, cluster size > 48 . Brain regions that showed significant changes are described in Table 3. Abbreviations: tDCS, transcranial direct current stimulation; DC, degree centrality; Ab, amyloid beta

Supplementary Files

This is a list of supplementary files associated with this preprint. Click to download.

- [SupplementaryMaterial.docx](#)